


CASE REPORT

Open Access

# $^{11}\text{C}$ -UCB-J synaptic PET and multimodal imaging in dementia with Lewy bodies



Nicolas Nicastro<sup>1,2\*</sup> , Negin Holland<sup>3</sup>, George Savulich<sup>1</sup>, Stephen F. Carter<sup>1</sup>, Elijah Mak<sup>1</sup>, Young T. Hong<sup>3,4</sup>, Selena Milicevic Sephton<sup>4</sup>, Tim D. Fryer<sup>3,4</sup>, Franklin I. Aigbirhio<sup>3,4</sup>, James B. Rowe<sup>3†</sup> and John T. O'Brien<sup>1†</sup>

\* Correspondence: [nicolas.nicastro@hcuge.ch](mailto:nicolas.nicastro@hcuge.ch)

<sup>†</sup>James B. Rowe AND John T. O'Brien have joint senior authorship.

<sup>1</sup>Department of Psychiatry, University of Cambridge, Cambridge, UK

<sup>2</sup>Division of Neurology, Department of Clinical Neurosciences, Geneva University Hospitals, 4 rue G. Perret-Gentil, 1205 Geneva, Switzerland

Full list of author information is available at the end of the article

## Abstract

**Objective:** Dementia with Lewy bodies (DLB) is a common cause of dementia, but atrophy is mild compared to Alzheimer's disease. We propose that DLB is associated instead with severe synaptic loss, and we test this hypothesis in vivo using positron emission tomography (PET) imaging of  $^{11}\text{C}$ -UCB-J, a ligand for presynaptic vesicle protein 2A (SV2A), a vesicle membrane protein ubiquitously expressed in synapses.

**Methods:** We performed  $^{11}\text{C}$ -UCB-J PET in two DLB patients (an amyloid-negative male and an amyloid-positive female in their 70s) and 10 similarly aged healthy controls. The DLB subjects also underwent PET imaging of amyloid ( $^{11}\text{C}$ -PiB) and tau ( $^{18}\text{F}$ -AV-1451).  $^{11}\text{C}$ -UCB-J binding was quantified using non-displaceable binding potential ( $\text{BP}_{\text{ND}}$ ) determined from dynamic imaging. Changes in  $^{11}\text{C}$ -UCB-J binding were correlated with MRI regional brain volume,  $^{11}\text{C}$ -PiB uptake and  $^{18}\text{F}$ -AV-1451 binding.

**Results:** Compared to controls, both patients had decreased  $^{11}\text{C}$ -UCB-J binding, especially in parietal and occipital regions (FDR-corrected  $p < 0.05$ ). There were no significant correlations across regions between  $^{11}\text{C}$ -UCB-J binding and grey matter, tau ( $^{18}\text{F}$ -AV1451) or amyloid ( $^{11}\text{C}$ -PiB) in either patient.

**Conclusions:** Quantitative imaging of in vivo synaptic density in DLB is a promising approach to understanding the mechanisms of DLB, over and above changes in grey matter volume and concurrent amyloid/tau deposition.

**Keywords:** Synaptic imaging, Dementia, Lewy bodies, Amyloid, Tau, Brain atrophy

## Introduction

Dementia with Lewy bodies (DLB) is a major cause of neurodegenerative dementia. It is characterized by recurrent visual hallucinations, parkinsonism, cognitive fluctuations and REM sleep behaviour disorder (McKeith et al., 2017). In contrast to clinical impairments, atrophy is typically mild in DLB compared to Alzheimer's disease (AD). Instead, the severity of disease may arise from a severe loss of synapses. Autopsy findings in DLB include alpha-synuclein deposition in association with loss of synaptic proteins (Berezcki et al., 2016; Bajic et al., 2012). Synaptic density can be estimated in vivo from the synaptic vesicle protein 2A (SV2A, a vesicle membrane protein ubiquitously expressed in synapses) using the radioligand  $^{11}\text{C}$ -UCB-J with positron emission

tomography (PET) (Nabulsi et al., 2016). In other degenerative disorders including AD, progressive supranuclear palsy and corticobasal degeneration, widespread reduction in  $^{11}\text{C}$ -UCB-J binding is observed, more so in disease-specific regions and in relation to clinical severity (Chen et al., 2018; Mecca et al., 2020; Holland et al., 2020).

In this case study,  $^{11}\text{C}$ -UCB-J PET imaging was assessed in two patients with probable DLB, with and without concurrent amyloid and tau deposition. We tested for differences in  $^{11}\text{C}$ -UCB-J binding between DLB and controls and assessed regional correlation of  $^{11}\text{C}$ -UCB-J binding with atrophy, PET imaging of amyloid ( $^{11}\text{C}$ -Pittsburgh compound B (PiB)) and tau ( $^{18}\text{F}$ -AV1451).

## Material and methods

### Patients inclusion

We included two patients with probable DLB: (1) a male presenting with a 5-year history of cognitive impairment (revised Addenbrooke's Cognitive Evaluation (ACER) score 81/100) interfering with daily activities, in association with cognitive fluctuations, REM sleep behaviour disorder and parkinsonism (Movement Disorders Society – Unified Parkinson's Disease Rating Scale (MDS-UPDRS) part III 27/132) and (2) a female presenting with a 2-year cognitive impairment (ACER 50/100) associated with cognitive fluctuations, visual hallucinations and parkinsonism (MDS-UPDRS III 13/132). Patients were recruited from specialist memory clinics in and around Cambridgeshire, the Dementias and Neurodegeneration specialty of the UK Clinical Research Network (DeNDRoN) or the Join Dementia Research (JDR) platform ([www.joindementiaresearch.nihr.ac.uk](http://www.joindementiaresearch.nihr.ac.uk)). Probable DLB was defined by the 2017 consensus criteria (McKeith et al., 2017).

Both patients underwent PET imaging with  $^{11}\text{C}$ -UCB-J,  $^{11}\text{C}$ -PiB and  $^{18}\text{F}$ -AV1451, as well as structural magnetic resonance imaging (MRI) (Bevan-Jones et al., 2017). They were compared to ten similarly aged control subjects, who were recruited from the JDR and local registers. Healthy controls had MMSE > 26, no cognitive symptoms, unstable/significant medical history or MRI contraindications.

### PET and MRI imaging acquisition and preprocessing

All radioligands were prepared at the Wolfson Brain Imaging Centre, University of Cambridge (Milicevic-Sephton et al., 2020).  $^{11}\text{C}$ -UCB-J PET imaging (mean injected activity: 368 MBq controls; 325 MBq DLB cases) used dynamic scanning for 90 min on a GE SIGNA PET/MR (GE Healthcare, Waukesha, USA), with attenuation correction including the use of a multi-subject atlas method (Burgos et al., 2014; Wu & Carson, 2002). For the DLB patients only, additional static  $^{11}\text{C}$ -PiB (550 MBq) and dynamic  $^{18}\text{F}$ -AV-1451 (370 MBq) PET scans were performed. Each emission image series was aligned using SPM12 (<https://www.fil.ion.ucl.ac.uk/spm/software/spm12>) to ameliorate the impact of patient motion during data acquisition and then rigidly registered to the corresponding T1-weighted MRI image. The Hammersmith atlas (<http://brain-development.org/brain-atlases>) regions of interest (ROIs) were non-rigidly registered to each T1-weighted MRI image. Regional time-activity curves were corrected for cerebrospinal fluid partial volume using SPM12 tissue probability maps smoothed to PET spatial resolution.  $^{11}\text{C}$ -UCB-J non-displaceable binding potential ( $\text{BP}_{\text{ND}}$ ) was determined using a basis function implementation of the simplified reference tissue model (Wu & Carson, 2002), with the reference

tissue defined in the centrum semiovale (Koole et al., 2019). Regional  $^{11}\text{C}$ -PiB standardized uptake value ratio (SUVR) was determined using cerebellar grey matter as the reference tissue, which was also used as the reference region for  $^{18}\text{F}$ -AV-1451  $\text{BP}_{\text{ND}}$  quantified using a basis function simplified reference tissue model.

MRI imaging used a 3T scanner (MAGNETOM Trio; Siemens Healthineers, Erlangen, Germany) including a magnetization-prepared rapid gradient echo (MPRAGE) T1-weighted sequence (repetition time = 2300 ms, echo time = 2.98 ms, field of view =  $240 \times 256 \text{ mm}^2$ , 176 slices, flip angle =  $9^\circ$ , isotropic 1 mm voxels). Grey matter volume was assessed by volume-based morphometry (VBM) with Computational Anatomy Toolbox 12 (CAT12) using the standard pipeline (<http://www.neuro.uni-jena.de/cat>) (Dahnke et al., 2013). Images were smoothed with the recommended 8 mm–full-width at half maximum Gaussian kernel and regional values were extracted from the Hammersmith atlas.

### Statistical analysis

ROI-based comparison of  $^{11}\text{C}$ -UCB-J  $\text{BP}_{\text{ND}}$  and VBM data between the two DLB subjects (1/2 (50%) male, mean age 73 years) and 10 similarly aged controls (5/10 (50%) male, age mean  $\pm$  SD  $72.4 \pm 3.4$  years) was performed using a general linear model with repeated measure ANCOVA using age, sex and years of education as covariates. As 33 cortical and subcortical ROIs were assessed, we used a false discovery rate (FDR)-corrected  $p < 0.05$  with  $Q = 0.15$ . Subsequently, regional Z-scores for  $^{11}\text{C}$ -UCB-J  $\text{BP}_{\text{ND}}$ ,  $^{11}\text{C}$ -PiB SUVR,  $^{18}\text{F}$ -AV1451  $\text{BP}_{\text{ND}}$  and VBM data were computed for the DLB subjects by comparing them to the control group. Region-by-region correlations between the different brain imaging modalities were performed for the DLB subjects using Spearman correlations.

### Results

The first DLB patient (74-year-old male) was amyloid-negative (average neocortical  $^{11}\text{C}$ -PiB SUVR = 1.3), while the second patient (72-year-old female) was amyloid-positive (SUVR = 1.9). For  $^{11}\text{C}$ -UCB-J, there were significant group ( $p = 0.0012$ ), region ( $p < 0.0001$ ) and group  $\times$  region interaction effects ( $p < 0.0001$ ). Pairwise regional comparisons revealed decreased  $^{11}\text{C}$ -UCB-J  $\text{BP}_{\text{ND}}$  for both DLB patients compared to controls in extensive cortical regions (10/33 regions) and thalamus, with more prominent changes in parieto-occipital, middle and superior frontal cortices (FDR-corrected  $p < 0.05$ ) (Fig. 1). Similar results were obtained using non-partial-volume-effect corrected data.  $^{11}\text{C}$ -UCB-J time-activity curves in the reference region (centrum semiovale) were similar among groups (Supp. Figure 1). Of note, we did not observe any significant differences between DLB and controls in the deep brain nuclei, except for the thalamus (FDR-corrected  $p < 0.05$ ).

VBM analysis of regional volumes showed a significant effect of region ( $p < 0.0001$ ) but no significant effect of group ( $p = 0.17$ ) or group  $\times$  region interaction ( $p = 0.20$ ). In addition, we observed that  $^{11}\text{C}$ -UCB-J  $\text{BP}_{\text{ND}}$  Z-scores for DLB subjects were lower compared to VBM Z-scores. For example, in the superior frontal gyrus,  $^{11}\text{C}$ -UCB-J Z-

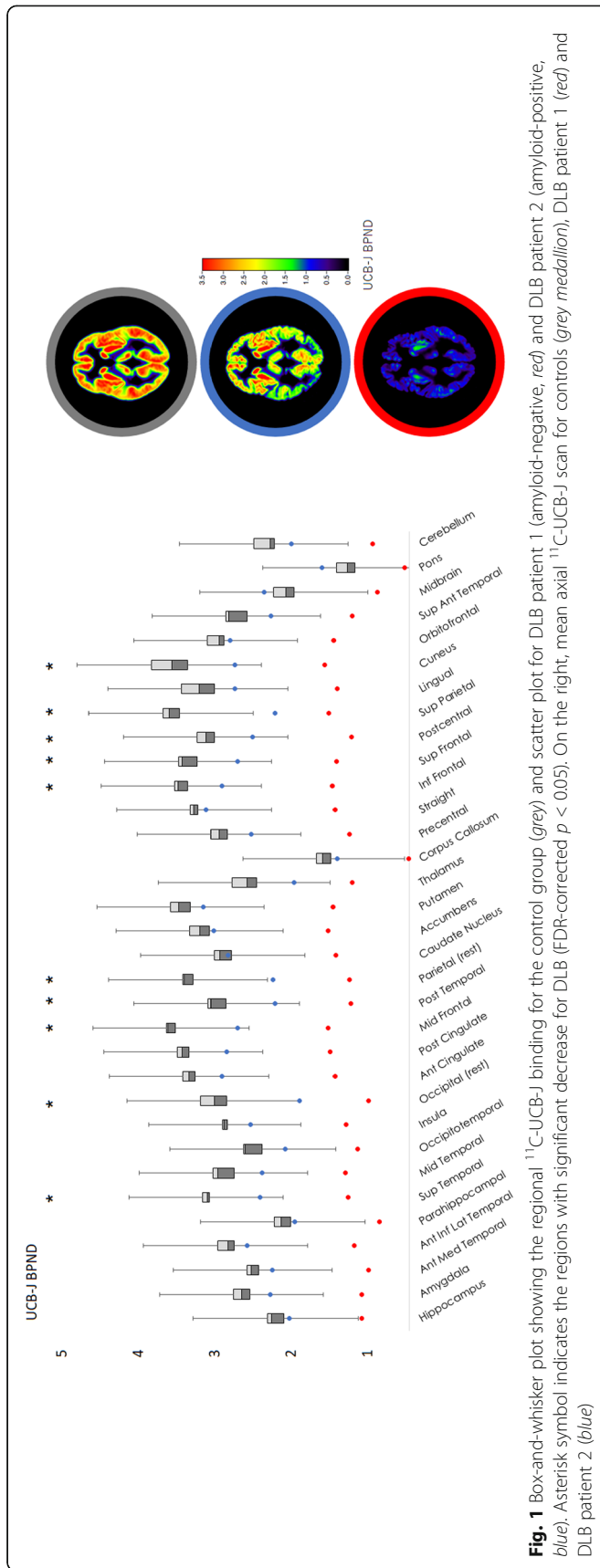


**Fig. 1** Box-and-whisker plot showing the regional <sup>11</sup>C-UCB-J binding for the control group (grey) and scatter plot for DLB patient 1 (amyloid-negative, red) and DLB patient 2 (amyloid-positive, blue). Asterisk symbol indicates the regions with significant decrease for DLB (FDR-corrected  $p < 0.05$ ). On the right, mean axial <sup>11</sup>C-UCB-J scan for controls (grey), DLB patient 1 (red) and DLB patient 2 (blue)

score was  $-1.7$  while grey matter atrophy  $Z$ -score was  $-0.4$ . Similarly,  $^{11}\text{C}$ -UCB-J  $\text{BP}_{\text{ND}}$   $Z$ -score in lingual gyrus was  $-1.5$  whereas VBM  $Z$ -score was  $-0.7$ .

Region-by-region correlations for the DLB patients showed no significant correlation between  $^{11}\text{C}$ -UCB-J  $\text{BP}_{\text{ND}}$  and grey matter volume ( $\rho = 0.24$ ,  $p = 0.17$  for DLB patient 1 and  $\rho = 0.27$ ,  $p = 0.13$  for DLB patient 2). No significant correlation was observed between  $^{11}\text{C}$ -PiB SUVR and UCB-J  $\text{BP}_{\text{ND}}$  (both patients  $p > 0.3$ ).  $^{18}\text{F}$ -AV1451  $\text{BP}_{\text{ND}}$  and  $^{11}\text{C}$ -UCB-J  $\text{BP}_{\text{ND}}$  did not correlate in either patient ( $p > 0.10$ ).

## Discussion

The present study indicates marked synaptic loss in DLB using  $^{11}\text{C}$ -UCB-J PET. Reduced  $^{11}\text{C}$ -UCB-J binding was evident in posterior cortical regions after partial volume effect correction and so represented a change beyond that of brain atrophy. This demonstrates markedly reduced SV2a density in DLB. Further studies are needed at earlier prodromal stage to understand the progression of synaptic loss in DLB.

Previous findings in MCI and early AD indicated synaptic loss restricted to the hippocampus (Chen et al., 2018), while in AD decreases in  $^{11}\text{C}$ -UCB-J binding were found in the hippocampus, amygdala, thalamus, cingulate and temporal lobe (Venkataraman, 2019). Recently, widespread synaptic loss was observed in cortical and subcortical regions for 4-R tauopathies (Holland et al., 2020). Toyonaga et al. showed that in an amyloid precursor protein and presenilin 1 double transgenic mice model of AD,  $^{11}\text{C}$ -UCB-J baseline PET exhibited decreased hippocampal synaptic density, while the follow-up scan after treatment with saracatinib (a dual kinase inhibitor) revealed a significant increase in hippocampal synaptic density (Toyonaga et al., 2019). These findings suggest that  $^{11}\text{C}$ -UCB-J could be a valuable marker of disease severity and treatment monitoring for future therapeutic trials in human.

Regarding Parkinson's disease (PD), Matuskey et al. recently showed that a significant (17–41%) reduction of  $^{11}\text{C}$ -UCB-J binding was observed for mild-moderate PD in deep nuclei (substantia nigra, red nucleus, locus coeruleus) and parahippocampal gyrus (Matuskey et al., 2020). For the present study, our DLB did not show any significant changes in synaptic density in deep brain nuclei, except for the thalamus. However, it is worth mentioning that we performed correction for multiple comparisons, which was not the case for the study by Matuskey et al.

In our two cases, we did not observe correlations between regional  $^{11}\text{C}$ -UCB-J  $\text{BP}_{\text{ND}}$  and regional atrophy, suggesting that our assay of synaptic loss is not merely an index of volume loss. Regional synaptic density loss was also not associated with amyloid ( $^{11}\text{C}$ -PiB) or tau ( $^{18}\text{F}$ -AV1451) in both DLB patients, suggesting that the synaptic ligand is informative over synaptic aspects of pathogenesis over and above the information obtained from amyloid and tau imaging.

Our study has limitations, including the inclusion of a case and replication rather than a large cohort. In addition, the synaptic PET was obtained after the tau and amyloid PET, and we cannot exclude progression of pathology even in the absence of a significant progression of the clinical severity. Moreover, arterial input function was not performed during the acquisition of PET imaging. We also rely on clinical diagnostic criteria and do not have pathological confirmation of DLB pathology.

## Conclusions

In summary, we report that the binding of  $^{11}\text{C}$ -UCB-J—an in vivo marker of synaptic density—was markedly decreased in two well-characterized DLB patients. Further studies are required to assess whether such changes are characteristic of DLB, to correlate synaptic loss with key symptoms and to monitor change over time from prodromal through to established dementia in order to improve our understanding of pathophysiological processes involved in neurodegeneration.

## Supplementary Information

The online version contains supplementary material available at <https://doi.org/10.1186/s41824-020-00093-9>.

**Additional file 1: Supplementary Figure 1.**  $^{11}\text{C}$ -UCB-J time-activity curves in the reference region.

## Abbreviations

ACER: Addenbrooke's Cognitive Evaluation Revised; AD: Alzheimer's disease; BPND: Non-displaceable binding potential; CAT12: Computational Anatomy Toolbox 12; DLB: Dementia with Lewy bodies; FDR: False discovery rate; MDS-UPDRS: Movement Disorders Society Unified Parkinson Disease Rating Scale; MRI: Magnetic resonance imaging; PiB: Pittsburgh compound B; PET: Positron emission tomography; SUVR: Standardized uptake value ratio; SV2A: Synaptic vesicle 2A

## Acknowledgements

We are grateful to our DLB patients and control subjects for their participation in the study. We thank the radiographers at the Wolfson Brain Imaging Centre and PET/CT Unit, Addenbrooke's Hospital, Cambridge, UK, for their support in data acquisition, together with Dr Roido Manavaki for her contribution to the PET/MR attenuation correction methods used. We thank UCB for supplying the precursor for the manufacturing of  $^{11}\text{C}$ -UCB-J for use in this study.

## Authors' contributions

Conceptualisation: JBR, JTOB and FIA; methodology: NN, YTH, TDF, JBR and JTOB; investigation: NN, NH and GS; formal analysis: NN; resources: FIA. Writing: original draft: NN; review and editing: NH, GS, SFC, EM, YTH, SMS, TDF, FIA, JBR and JTOB; funding acquisition: JBR and JTOB; supervision: JBR, JTOB and FIA. The author(s) read and approved the final manuscript.

## Funding

The study was funded by the NIHR Cambridge Biomedical Research Centre and MRC; Wellcome Trust (103838); the Cambridge Centre for Parkinson's Plus Centre; Alzheimer Research UK; the Association of British Neurologists, Patrick Berthoud Charitable Trust (RG99368).

## Availability of data and materials

The datasets used and analysed during the current study are available from the corresponding author on reasonable request.

## Ethics approval and consent to participate

The East of England institutional review boards approved the NIMROD (13/EE/0104), TENDER (16/EE/0529) and SENDER (18/EE/0059) protocols and written informed consent was obtained from all participants prior to inclusion.

## Consent for publication

All subjects included in the present study have signed a consent form for publication.

## Competing interests

N. N., N.H., G.S., S.F.C., E.M., Y.T.H., S.M.S. and T.D.F. declare that they have no conflict of interests. F.I.A. received academic grant support from GE Healthcare and served as a consultant for Avid and Cantabio, all for matters not related to the current study. J.B.R. has been a consultant for Asceneuron and Syncona and has received academic grant funding from AZ-MedImmune, Janssen and Lilly, unrelated to this study. J.T.O. reports personal fees from TauRx, personal fees from Axon, personal fees from GE Healthcare, grants and personal fees from Avid/Lilly, personal fees from Eisai, grants from Alliance Medical, personal fees from Roche and grants from Merck, outside the submitted work.

## Author details

<sup>1</sup>Department of Psychiatry, University of Cambridge, Cambridge, UK. <sup>2</sup>Division of Neurology, Department of Clinical Neurosciences, Geneva University Hospitals, 4 rue G. Perret-Gentil, 1205 Geneva, Switzerland. <sup>3</sup>Department of Clinical Neurosciences, University of Cambridge, Cambridge, UK. <sup>4</sup>Wolfson Brain Imaging Centre, University of Cambridge, Cambridge, UK.

Received: 1 July 2020 Accepted: 15 November 2020

Published online: 22 December 2020

## References

- Bajic N, Jenner P, Ballard CG, Francis PT (2012) Proteasome inhibition leads to early loss of synaptic proteins in neuronal culture. *J Neural Transm (Vienna)* 119(12):1467–1476
- Berezcki E, Francis PT, Howlett D et al (2016) Synaptic proteins predict cognitive decline in Alzheimer's disease and Lewy body dementia. *Alzheimers Dement* 12(11):1149–1158
- Bevan-Jones WR, Surendranathan A, Passamonti L et al (2017) Neuroimaging of inflammation in memory and related other disorders (NIMROD) study protocol: a deep phenotyping cohort study of the role of brain inflammation in dementia, depression and other neurological illnesses. *BMJ Open* 7(1):e013187
- Burgos N, Cardoso MJ, Thielemans K et al (2014) Attenuation correction synthesis for hybrid PET-MR scanners: application to brain studies. *IEEE Trans Med Imaging* 33(12):2332–2341
- Chen MK, Mecca AP, Naganawa M et al (2018) Assessing synaptic density in Alzheimer disease with synaptic vesicle glycoprotein 2A positron emission tomographic imaging. *JAMA Neurol* 75(10):1215–1224
- Dahnke R, Yotter RA, Gaser C (2013) Cortical thickness and central surface estimation. *Neuroimage* 65:336–348
- Holland N, Jones PS, Savulich G, et al. Synaptic loss in primary tauopathies revealed by (11C)-UCB-J positron emission tomography. *Mov Disord* 2020 (in press)
- Koole M, van Aalst J, Devrome M et al (2019) Quantifying SV2A density and drug occupancy in the human brain using [(11)C]UCB-J PET imaging and subcortical white matter as reference tissue. *Eur J Nucl Med Mol Imaging* 46(2):396–406
- Matuskey D, Tinaz S, Wilcox KC et al (2020) Synaptic changes in Parkinson disease assessed with in vivo imaging. *Ann Neurol* 87:329–338
- McKeith IG, Boeve BF, Dickson DW et al (2017) Diagnosis and management of dementia with Lewy bodies: fourth consensus report of the DLB consortium. *Neurology* 89(1):88–100
- Mecca AP, Chen MK, O'Dell RS, et al. In vivo measurement of widespread synaptic loss in Alzheimer's disease with SV2A PET. *Alzheimers Dement* 2020.
- Milicevic-Sephton S, Miklovicz T, Russell JJ et al (2020) Automated radiosynthesis of (11C)-UCB-J for imaging synaptic density by positron emission tomography. *J Labelled Comp Radiopharm* 63(3):151–158
- Nabulsi NB, Mercier J, Holden D et al (2016) Synthesis and preclinical evaluation of 11C-UCB-J as a PET tracer for imaging the synaptic vesicle glycoprotein 2A in the brain. *J Nuclear Med* 57(5):777–784
- Toyonaga T, Smith LM, Finnema SJ et al (2019) In vivo synaptic density imaging with (11)C-UCB-J detects treatment effects of saracatinib (AZD0530) in a mouse model of Alzheimer's disease. *J Nucl Med* 60(12):1780–1786
- Venkataraman A (2019) The Niels Lassen award session and Oral sessions. *J Cereb Blood Flow Metab* 39(1\_suppl):1–123
- Wu Y, Carson RE (2002) Noise reduction in the simplified reference tissue model for neuroreceptor functional imaging. *J Cereb Blood Flow Metab* 22(12):1440–1452

## Publisher's Note

Springer Nature remains neutral with regard to jurisdictional claims in published maps and institutional affiliations.

Submit your manuscript to a SpringerOpen<sup>®</sup> journal and benefit from:

- Convenient online submission
- Rigorous peer review
- Open access: articles freely available online
- High visibility within the field
- Retaining the copyright to your article

Submit your next manuscript at ► [springeropen.com](https://www.springeropen.com)